CONTINUAL DETERMINATION OF MAGNITUDE FOR EARTHQUAKE EARLY WARNING

Qiang MA [1] and Xing JIN [1,2]

[1] *Associate Researcher, Dept. of Engineering Seismology & Strong Motion Observation, Institute of Engineering Mechanics, Harbin. China*

[2] *Researcher, Earthquake Administration of Fujian Province, Fuzhou, China*
Email: maqiang@iem.net.ac

ABSTRACT :

Earthquake early warning (EEW) system can detect actual quakes near their source and issue warnings to humans and automated systems for specific region to mitigate disaster. Rapid determination of the location and magnitude of an earthquake are two fundamental problems for early earthquake detection and warning systems. We develop a method to determinate the magnitude continually for every second after 1sec of the nearest station P-wave arrival using the seismic network records. Various natural periods' single-degree-of-freedom system response of acceleration, velocity and displacement are obtained using real-time simulation method and the different frequency band is considered. Three predomination period parameters and three amplitude parameters based on different frequency band records are proved effective to determinate magnitude. The six parameters are effective cumulative ascending pulse width of first displacement pulse, V_{max}/A_{max} period, "predominant period τ_c", PGA, PGV and PGD respectively within a certain short time segment after the P-wave arrival. The neural network is used to model the nonlinear relation between the magnitude and all the six parameters for different frequency band for every second after the P wave arrival. The neural network is trained and the result shows that the method is effective and reliable to determinate the magnitude for EEW.

KEYWORDS: Earthquake early warning, Magnitude, Neural networks

1. INTRODUCTION

Earthquake early warning (EEW) systems hold the potential to reduce the damaging affects of earthquakes by giving a few seconds to a few tens of seconds warning before the arrival of damaging ground motion. The concept of EWS was proposed by Cooper(1868), and along with the development of earthquake observation, data transmission and the computer technology, a model for a seismic computerized alert network (SCAN) was advanced by Heaton (1985). Nowadays many early warning systems using a network of seismic instruments to determine earthquake magnitude and location has developed in many countries and regions like Japan, Mexico, Taiwan Region, Turkey and so on (Nakamura,1988; Espinosa-Aranda et al., 1995; Wu et al., 1998; Wu and Teng, 2002; Allen and Kanamori, 2003; Kamigaichi, 2004;). In Japan, the Urgent Earthquake Detection and Alarm System (UrEDAS) (Nakamura, 1988) has been used in railway alarm systems and the EEW system (or Kinkyu Jishin Sokuho in Japanese) that can estimate seismic intensities and expected arrival time of principal motion has been used in the whole country (Kamigaichi, 2004; Horiuchi et al., 2005).
Rapidly determination of earthquake magnitude in the few to tens of seconds before the damaging ground motion occurs is very importance for EEW system. In order to provide real-time magnitude estimations for EEW purposes, lots of methods have been developed. A method based on the predominant period (τ_c) of the P-wave has been proposed (Nakamura 1988, Allen and Kanamori, 2003; Lockman and Allen, 2005; Olson and Allen 2005). Rydelek and Horiuchi (2006) used the predominant period to look for a scaling relation from the records of Japanese Hi-net seismic network but were unable to identify a relation similar to the result of Olson and Allen (2005) who used the datasets in southern California. Wolfe (2006) has also explored the properties of the predominant period observation identifying limitations to the methodology that introduce errors into the observations. Simons et al. (2006) develop an alternative approach to measure predominant period using wavelet multiscale analysis. Grecksch and Kumpel (1997) demonstrated that the first second of the P wave can be used to estimate the magnitude within 0.5 magnitude units by using records of strong motion sensors. Wu

(2006) demonstrated that the peak amplitude of displacement in the first three seconds after the arrival of the P wave can be used to estimate the '*Pd* magnitude' , for earthquakes in southern California the *Pd* magnitudes agree with the catalog magnitudes with a standard deviation of 0.18 for events less than magnitude 6.5.
In the interest of improving the precision and the stability for the estimation of magnitude for EEW, we developed another continual determination method of magnitude. Various period parameters and amplitude parameters for different frequency band include peak acceleration, peak velocity, peak displacement, predominant period (τ_c), the ratio of peak velocity and peak acceleration V_{max}/A_{max}, and effective cumulative ascending pulse width of first displacement pulse for every second after P-wave arrival were considered. All the parameters of different frequency band were synthesized using Artificial Neural Networks (ANN). So, various characters of every initial P-wave segment were considered synthetically and continuously. We test our method on the bedrock records of digital strong-motion seismograph of Japan (KiK-net). The result shows that the magnitude of the single station for every second after the P-wave arrival is satisfying for EEW.

2. DATASETS

In the present study we used borehole records from Strong Motion Seismograph networks (Kiban Kyoshin network, Kik-net) of Japan. The borehole was design so that it penetrates the sediment and reaches to rock. The selection criteria were Mj>4.0 and the records at the hypocentral distance that satisfied the following Eqn.2.1

$$\log R \leq 0.86 + 0.17 M_j \tag{2.1}$$

A total of 141 events and 1018 three-component records occurred during the period from 1997 to 2007 that were widely felt in Japan were used for this study (Fig. 1 and Fig. 2). Based on the introduction of Aoi and Kunugi (2004), the sensor being used is a V403 or V404 tri-axial force-balance accelerometer with a natural frequency of 450 Hz and a damping factor of 0.707. The typical sensor gain is 3 V/g (0.306 V/m/s^2). The data loggers used SMAC-MDK that they have a 24-bit A/D (effective resolution is at least 18-bit) converter and a maximum measurable acceleration of 2000 gals (cm/s^2). Waveforms are recorded with a sampling rate of 200 Hz.

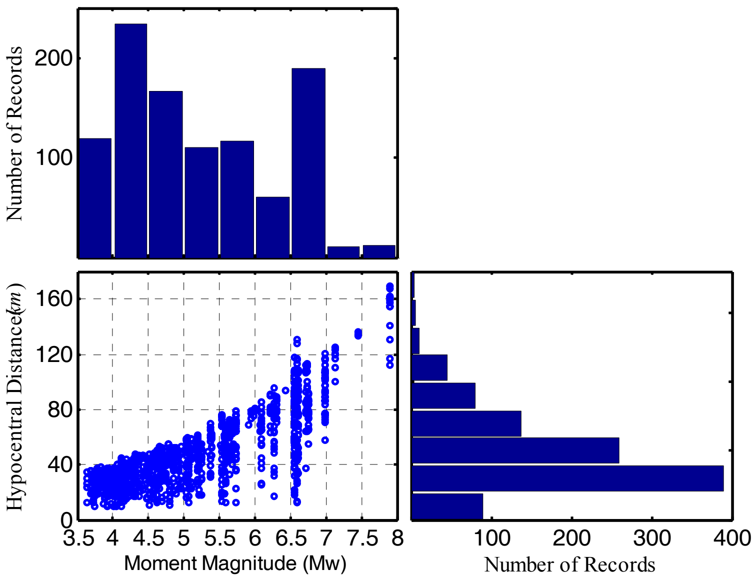

Figure 1 Data distribution *vs.* moment magnitude and hypocentral distance (bottom left). Histogram of the number of selected strong motion records with moment magnitude (top). Histogram of the number of selected strong motion records with hypocentral distance (bottom right).

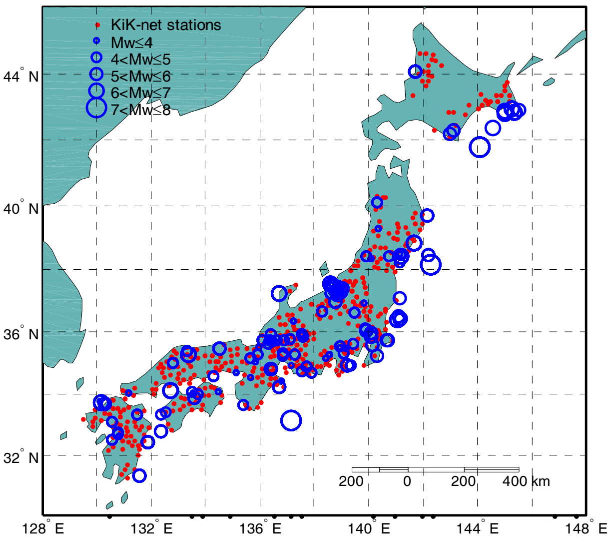

Figure 2 Map showing the locations of events (circles) and Kik-net stations (dot) used in this study

3. PERIOD AND AMPLITUDE PARAMETERS FOR EEW MAGNITUDE

Based on the research of 'predominant period (τ_c)' method (Nakamura 1988, Allen and Kanamori, 2003; Lockman and Allen, 2005; Olson and Allen 2005) and the '*Pd* magnitude' (Wu , 2006) . It showed that the magnitude can be estimated from the first several seconds after the arrival of the P wave, but the result had a large error for individual station.

3.1 'Predominant period' and 'Pd magnitude'

Using a total of 141 events and 1018 three-component records that referred before, the best-fit moment magnitude relation for 'predominant period (τ_c)' method (Allen and Kanamori, 2003) using the first 3sec of 141 events and 1018 vertical-component records as follows:

$$M_W = 7.088 + 4.202\log(Tp) \pm 0.900 \quad (3.1)$$

here *Tp* is the predominant period within 3s after the P-wave arrival that can be got in real-time algorithm. The standard deviation (SE) in the moment magnitude estimate is 0.90 for individual station waveform (Fig.3).

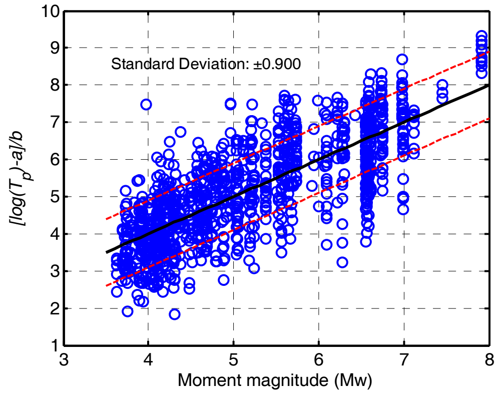

Figure 3. Correlation between actual moment magnitude and the moment magnitude estimated by maximum predominant period observed within 3s of the P-wave arrival for individual stations for a total of 141 events and 1018 vertical-component records.

The best-fit moment magnitude relation using the peak acceleration amplitude(PGA), peak velocity amplitude(PGV) and peak displacement amplitude(PGD) of the first 3sec P-wave for 141 events and 1018 vertical-component records as follows:

$$M_W = 1.931\log PGA_{P3} + 4.948\log(R+10) - 4.562 \pm 0.709 \quad (3.2\text{-}1)$$

$$M_W = 1.585\log PGV_{P3} + 3.417\log(R+10) + 0.643 \pm 0.597 \quad (3.2\text{-}2)$$

$$M_W = 1.460\log PGD_{P3} + 2.432\log(R+10) + 3.514 \pm 0.555 \quad (3.2\text{-}3)$$

here PGA_{P3}, PGV_{P3} and PGD_{P3} are the first 3s of the P-wave arrival for PGA, PGV and PGD, respectively, and R is the hypocentral distance. The standard deviation in the moment magnitude estimation is 0.709, 0.597 and 0.555 for PGA, PGV and PGD, respectively, for individual station waveform (Fig.4).

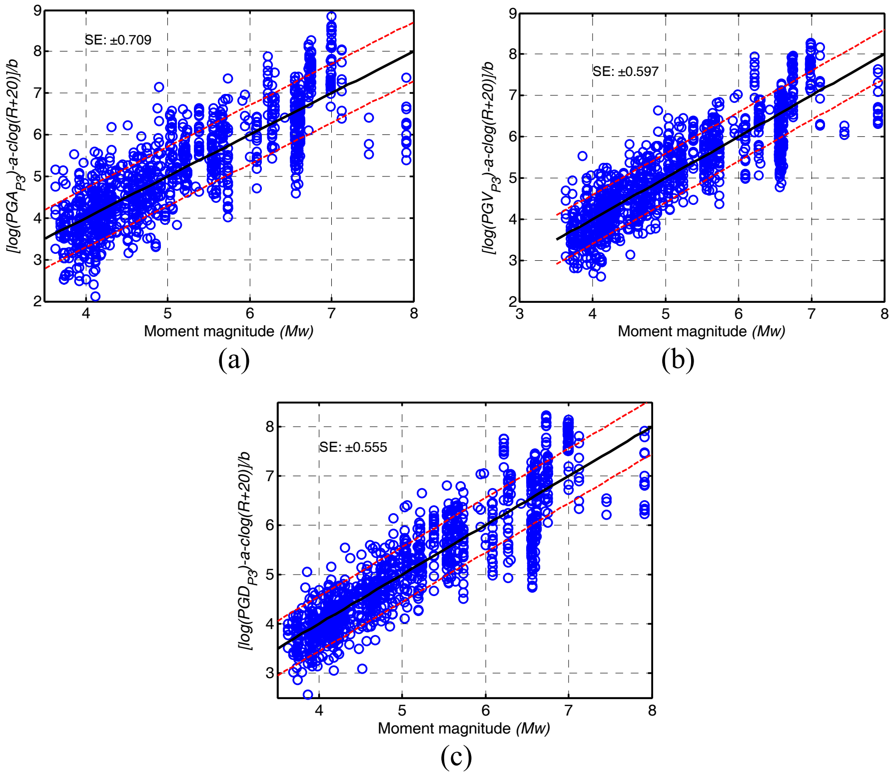

Figure 4. Correlation between actual moment magnitude and the moment magnitude estimated by (a) PGA, (b) PGV and (c) PGD, within 3s of the P-wave arrival for individual stations for a total of 141 events and 1018 vertical-component records.

3.2 Effective Cumulative Ascending Pulse Width

In general, for a point source, if the fault motion occurs over a duration of τ, then the near-field wave form is a ramp function and the far-field wave form is a pulse with a duration of τ . The relationship between seismic moment, M_0, and source duration, τ, provides information regarding the mechanics of faulting in the Earth's interior. The relation of M_0, and the pulse width of ground velocity or equivalently the rise time of the far-field displacement pulse, denoted by $\tau_{1/2}$, is approximately given by

$$M_0 \propto \tau_{1/2}{}^3 \quad (3.3)$$

For small earthquake (Fig.5) the first pulse of displacement is regular but for large earthquake (Fig.6) which has a complicated rupture process, the first pulse of displacement is irregular and we consider the pulse duration as several subevents as follows:

$$M_{0i} \propto \sum \tau_{i1/2}{}^3 \quad (3.4)$$

The effective cumulative ascending pulse width τ_e, defined as follows:

$$\tau_e = (\sum \tau_{i1/2}{}^3)^{1/3} \quad (3.5)$$

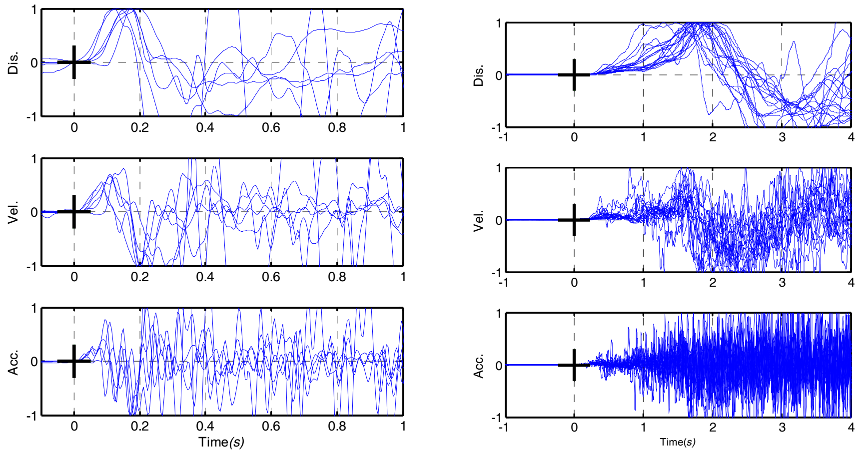

Figure 5 (Left)P-wave records of a small earthquake (*Mj*=4.0, *Mw*=3.7) scaled to maximum amplitude of first half-cycle of each signal (Top: Displacement, Middle: Velocity, Bottom: Acceleration)
Figure 6 (Right)P-wave records of a large earthquake (*Mj*=7.0, *Mw*=7.0) scaled to maximum amplitude of first half-cycle of each signal (Top: Displacement, Middle: Velocity, Bottom: Acceleration)

The onset of P-wave was automatically picked using the ratio of short time average to long time average (STA/LTA) and Akaike information criteria (AIC) picker. We used the first zero crossing of the seismic displacement signal to get the initial pulse width. When the onset of P-wave was obtained the velocity signal was considered to distinguish the pulse duration for every subevent. For example, if the first pulse of the displacement is positive, for the ascending segment of displacement the velocity is positive, for the extremum of displacement the velocity is zero and for descending segment the velocity is negative. Only the segments that the velocity is positive is considered as one subevent with the width $\tau_{i1/2}$ as shown in Eqn.3.5.
From this study, the effective cumulative ascending pulse width τ_e is found to be proportional to *Mw* in a simple manner. The best-fit relation using total of 141 events and 1018 vertical-component records as follows:

$$M_w = 7.196 + 4.673\log(\tau_e) \pm 0.864 \tag{3.6}$$

here τ_e is effective cumulative ascending pulse that showed in Eqn.3.5. The SE in the moment magnitude estimate is 0.864 for individual station waveform (Fig.7).

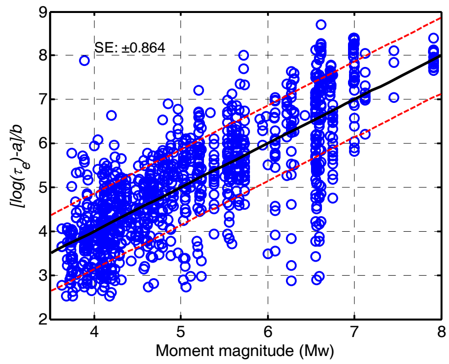

Figure 7. Correlation between actual moment magnitude and the moment magnitude estimated by effective cumulative ascending pulse width observed within 3s of the P-wave arrival for individual stations for a total of 141 events and 1018 vertical-component records.

4. ARTIFICIAL NEURAL NETWORK (ANN) FOR MAGNITUDE ESTIMATION

Based on the study of Wolf (2006) of ‘predominant period’ method as a estimator of magnitude for EEW, it pointed out that this estimator is a nonlinear function of spectral amplitude and period that gives greater weight

to higher amplitudes and higher frequencies in the spectrum and suggested that more detailed analyses into the magnitude dependence of the spectral characteristics of initial P-wave data, such as using multitaper spectral or wavelet approaches. Also these prior result in section 3 shows that although the 'predominant' period' and the amplitude within very short time of the P-wave arrival there is large discreteness for estimation of magnitude.
We use another method to consider the multi-estimator and the nonlinear of spectral amplitude, period and other parameters to estimate the magnitude on EEW. Various natural periods' single-degree-of-freedom system (SDOFs) response of acceleration, velocity and displacement are obtained using real-time simulation method and the different frequency band is considered. In this study, for SDOFs response are considered and the natural periods are 10s, 5s, 3s and 1s respectively, the damp ration is 0.707. For each band frequency the six parameters that they are effective cumulative ascending pulse width of first displacement pulse, V_{max}/A_{max} period, 'predominant period τ_c', PGA, PGV and PGD respectively within a certain short time segment after the P-wave arrival. Because peak velocity and peak acceleration are usually associated with the motions of different frequency. The ratio V_{max}/A_{max} should be related to the frequency content of the motion (McGurie, 1978). Now for every frequency band we have six estimators for magnitude and for four frequency bands and there are 24 estimators. The neural networks are used to model the nonlinear relation between the magnitude and all the six parameters for different frequency band and the hypocentral distance for every second after the P wave arrived. The sketch map for the train of neural networks is shown in Fig.8.

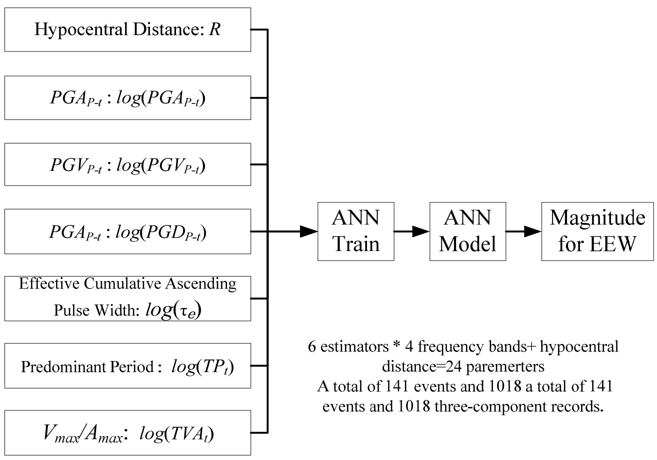

Figure 8 The sketch map for the train of neural networks. Where PGA_{P-t}, PGV_{P-t} and PGD_{P-t}, are the first t sec of the P-wave arrival for PGA, PGV and PGD, respectively.

A two-layer feed-forward network is used in this study. The input, hidden layer, output layer and output are shown in Fig.9. The early stopping training functions is used in the neural networks training to avoid the overfit the data. 1018 records are random divided into three subsets. The first subset of 60% datum is the training set, which is used for computing the gradient and updating the network weights and biases. The second subset of 20% datum is the validation set. The error on the validation set of 20% datum is monitored during the training process.

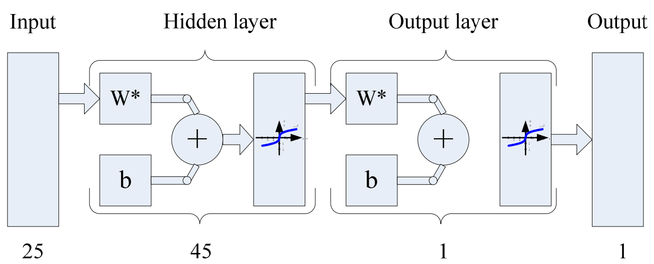

Figure 9. The layer diagram of the two-layer feed-forward network
with 45 hidden layer and 1 output layer.

4. RESULTS AND EXAMPLE

4.1 The results of estimation for magnitude

After getting the onset of P-wave automatically, 24 estimators within every second of the P-wave arrival are obtained until the S-wave arrival or 10s of the P-wave arrival for 1018 vertical-component records. And all the estimators with the hypocentral distance are trained using early stopping method.

The results within 1s and 3s of the P-wave arrival are shown in Fig.10 and Fig.11. And the results within every second point of the P-wave arrival are shown in Table 4.1

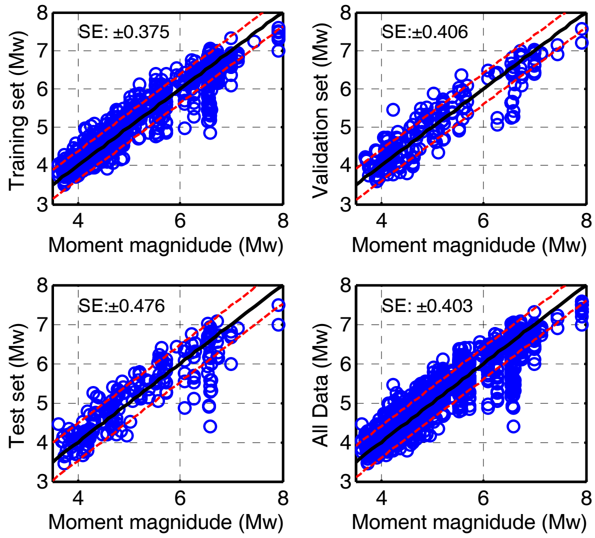

Figure 10 The results of magnitude using the ANN within 1s of the P-wave arrival for individual station.

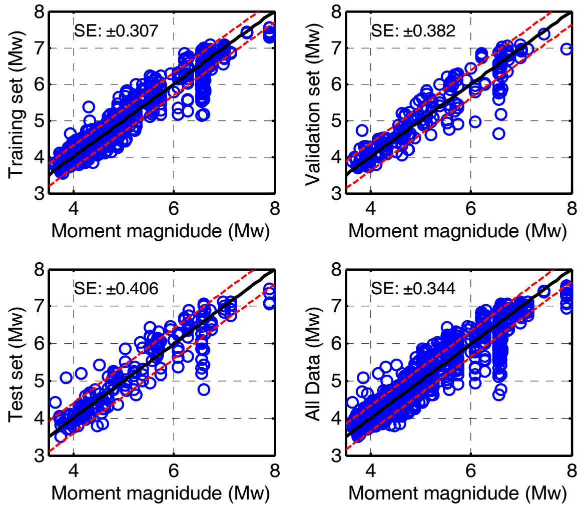

Figure 11 The results of magnitude using the ANN within 3s of the P-wave arrival for individual station.

Table 4.1The results within every second point of the P-wave arrival

Within *t* sec of the P-wave arrival	1s	2s	3s	4s	5s
Standard Deviation (SE)	0.403	0.334	0.344	0.266	0.244
Within *t* sec of the P-wave arrival	6s	7s	8s	9s	0s
Standard Deviation (SE)	0.271	0.280	0.266	0.243	0.275

4.2 Example of Continual Determination of Magnitude for Earthquake Early Warning

On October 23, 2004, an earthquake (Mw=6.6, Mj=6.8) occurred in Mid Niigata Pref., Honshu, Japan. The depth of hypocenter is 14km approximately. The location of event and 33 Kik-net stations that we used in this example are shown in Fig.12. Only the P-wave is used and the continual determination process of magnitude for earthquake early warning is shown in Fig.13 and Table 4.2. After 4.1 second of the earthquake occurred, the nearest KiK-net station NIGH12 received the 1sec P-wave and we can get the moment magnitude is 6.5, and the S-wave was not arrive to the ground at that moment.

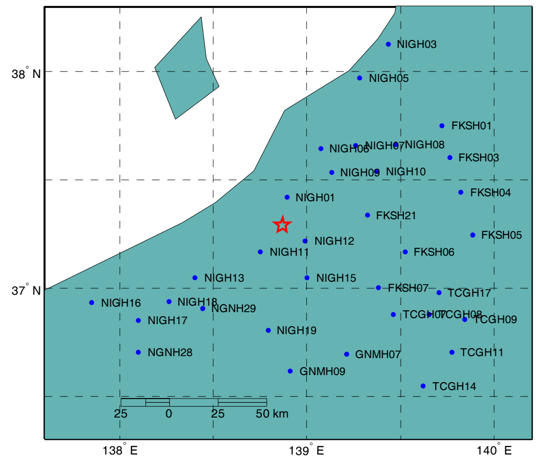

Figure 12 The location of Mid Niigata Pref. Earthquake of October 23, 2004 (star) and Kik-net stations (dot) used in this example

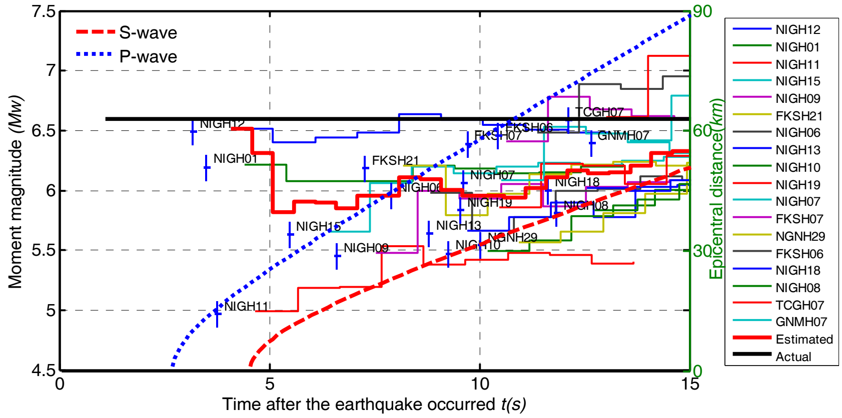

Figure 13 Continual determination process of magnitude for earthquake early warning (only P-wave is used)

5. DISCUSSION AND CONCLUSIONS

Large earthquakes in populated areas are potentially damaging. Therefore, it is very important for an earthquake alarm system to determine source parameters as quickly as possible. We developed a continual determination method of magnitude for EEW using multi-estimator in different frequency-band that they are synthesized by Artificial Neural Networks (ANN). We test our method on the bedrock records of digital strong-motion seismograph of Japan (KiK-net). Within only one minute after the nearest station P-wave arrival, the method can estimate the magnitude well. Along with more stations get more waveform information, the result continually be revised better and better commonly. So the method can be used to on-site warning as well as regional warning. The S-wave information is not used in this study to estimate the magnitude, if the S-wave of the station near the epicenter was used, the result should be better. As similar principle of magnitude real-time continuous determination, imminent damaging S-wave ground shaking and intensity also can be estimated within a very short P-wave arrived. Provided a dense array of networked seismometers exists, our procedure should become the tool of choice for earthquake early-warning systems.

Table 4.2 The continual determination process of magnitude for individual station (only P-wave is used)

Station Name	**R (km)**	**P Travel time (s)**	**The magnitude for individual station**									
			1s	**2s**	**3s**	**4s**	**5s**	**6s**	**7s**	**8s**	**9s**	**10s**
NIGH12	18.1	3.1	6.5	6.4	6.4	6.5	6.6	6.6	6.5	6.5	6.5	6.5
NIGH01	20.0	3.4	6.2	6.1	6.1	6.1	6.2	6.2	6.1	6.2	6.2	6.2
NIGH11	21.5	3.7	5.0	5.2	5.2	5.5	5.4	5.4	5.5	5.5	5.4	5.4
NIGH15	31.6	5.4	5.7	6.1	6.2	6.1	6.2	6.2	6.2	6.2	6.3	6.3
NIGH09	38.2	6.5	5.5	6.0	5.9	6.1	5.9	6.0	6.1	6.1	6.1	6.1
FKSH21	42.1	7.2	6.2	5.8	6.0	6.1	6.2	6.2	6.2	6.3	6.3	6.3
NIGH06	45.8	7.8	6.0	5.7	5.8	6.0	6.0	6.1	6.1	6.1	6.1	6.1
NIGH13	51.0	8.7	5.7	5.8	5.9	5.8	6.0	6.0	6.1	6.1	6.1	6.1
NIGH10	53.8	9.2	5.5	5.6	5.8	5.9	6.0	6.1	6.1	6.2	6.2	6.2
NIGH19	55.4	9.5	5.9	6.2	6.2	6.1	6.3	6.3	6.3	6.3	6.3	6.3
NIGH07	55.8	9.5	6.1	6.5	6.5	6.4	6.3	6.4	6.4	6.4	6.4	6.3
FKSH07	56.4	9.6	6.4	6.8	6.7	6.6	6.6	6.6	6.6	6.6	6.6	6.6
NGNH29	58.2	9.9	5.6	5.7	5.8	6.0	6.2	6.2	6.2	6.2	6.2	6.2
FKSH06	60.7	10.4	6.5	6.9	6.8	7.0	6.9	6.9	6.9	6.9	6.9	6.9
NIGH18	67.6	11.5	6.0	6.0	6.1	6.2	6.2	6.3	6.2	6.2	6.2	6.1
NIGH08	68.8	11.8	5.8	5.9	6.1	6.2	6.3	6.4	6.4	6.4	6.4	6.4
TCGH07	70.4	12.0	6.6	7.1	7.0	6.8	6.7	6.7	6.7	6.7	6.7	6.7
GNMH07	73.6	12.6	6.4	6.8	6.7	6.8	6.7	6.7	6.8	6.8	6.7	6.7
GNMH09	75.7	12.9	6.2	6.3	6.3	6.5	6.5	6.5	6.5	6.5	6.4	6.4
TCGH17	81.7	14.0	6.7	7.0	7.0	7.0	6.8	6.9	6.8	6.8	6.8	6.8
TCGH08	83.7	14.3	6.6	6.7	6.8	7.0	6.8	6.8	6.8	6.7	6.7	6.7
NIGH17	84.7	14.5	6.0	6.1	6.3	6.5	6.5	6.4	6.4	6.4	6.5	6.5
NIGH05	85.4	14.6	6.3	6.2	6.4	6.4	6.3	6.4	6.4	6.4	6.4	6.4
FKSH04	86.4	14.8	6.3	6.7	6.7	6.8	6.8	6.8	6.8	6.7	6.7	6.7
FKSH03	86.8	14.8	6.4	6.7	6.7	6.7	7.0	6.9	6.6	6.6	6.6	6.6
FKSH05	90.0	15.4	6.6	6.6	6.6	6.7	6.6	6.7	6.7	6.7	6.6	6.6
FKSH01	91.9	15.7	6.4	6.9	6.9	6.6	6.6	6.7	6.6	6.6	6.6	6.6
NGNH28	95.2	16.3	6.2	6.5	6.6	6.7	6.6	6.8	6.7	6.7	6.7	6.7
TCGH09	99.2	16.9	6.8	6.8	6.8	7.0	6.9	6.8	6.8	6.8	6.8	6.8
NIGH16	99.4	17.0	6.7	6.8	6.7	6.7	6.7	6.8	6.8	6.7	6.7	6.6
TCGH11	104.0	17.8	6.7	6.9	7.0	7.1	7.0	7.0	6.8	6.8	6.8	6.8
TCGH14	106.6	18.2	6.6	6.9	6.9	6.9	6.8	6.9	6.8	6.7	6.7	6.8
NIGH03	106.7	18.2	6.6	6.7	6.7	6.7	6.7	6.8	6.8	6.7	6.7	6.7

Remark: here R is hypocentral distance

6. ACKNOWLEDGMENTS

This research was supported by the Basic Science Research Foundation of Institute of Engineering Mechanics (2006B01) and the Key Projects in the National Science & Technology Pillar Program (2006BAJ06B07-03 and 2006BAJ03B03-01).

REFERENCE

Allen, R.M, Kanamori, H., (2003). The potential for earthquake early warning in southern California. *Science*, 300: 786-789

Aoi, S., Kunugi, T., and Fujiwara H.(2004).Strong-Motion Seismograph Network Operated by NIED: K-Net And KiK-net， *Journal of Japan Association for Earthquake Engineering*, Vol. 4, No. 3 (Special Issue)

Cooper, (1868). Letter to editor, *San Francisco Daily Evening Bulletin*, Nov.3, 1968

Espinosa-Aranda, J.M., A. Jimenez, G. Ibarrola, F. Alcantar, A. Aguilar, M. Inostroza and S. Maldonado, (1995). Results of the Mexico City early warning system. *11th World Conference of Earthquake Engineering*, Acapulco, Mexico.

Grecksch G, Kümpel H-J. (1997). Statistical analysis of strong-motion accelerograms and its application to earthquake early-warning systems. *Geophys. J. Int.* ,129: 113-123.

Heaton T.H. (1985). A model for a seismic computerized alert network. *Science* 228: 987-990

Horiuchi S, Negishi H, Abe K, et al. (2005). An Automatic Processing System for Broadcasting Earthquake Alarms. *Bulletin of the Seismological Society of America*. 2005, 95(2): 708-718.

Kamigaichi, O. (2004). JMA earthquake early warning, *Journal of Japan Association for Earthquake Engineering*, Vol.4, No.3 (special issue)

Nakamura, Y. (1988). On the urgent earthquake detection and alarm system (UrEDAS), *Proc. 9th World Conf. Earthq. Eng.* 7, 673-678.

Lockman, A.B., Allen, R.M. (2005). Single-Station Earthquake Characterization for Early Warning. *Bulletin of the Seismological Society of America*. 95(6): 2029-2039.

McGuire，R.K., (1978). Seismic ground motion parameter relations, Journal of the Geotechnical Engineering Division, *ASCE*, Vol.104, No. GT4, 481-490.

Olson, E. L. and Allen, R. M. (2005). The deterministic nature of earthquake rupture, *Nature,* 438, 212-215.

Rydelek P and Pujol J. (2004), Real-Time Seismic Warning with a Two-Station Subarray. *Bulletin of the Seismological Society of America*. 94(4): 1546-1550.

Simons, F.J, Dando, B.D.E., Allen, R.M. (2006), Automatic detection and rapid determination of earthquake magnitude by wavelet multiscale analysis of the primary arrival. *Earth and Planetary Science Letters*. 250: 214–223.

Wolfe, C.J. (2006). On the Properties of Predominant-Period Estimators for Earthquake Early Warning. *Bull. Seism. Soc. Am*. 2006, 96(5): 1961-1965.

Wu, Y. M., Shin, T. C., and Tsai, Y. B. (1998). Quick and reliable determination of magnitude for seismic early warning, *Bull. Seism. Soc. Am* 88, 1254-1259.

Wu, Y. M. and Teng, T. A. (2002). Virtual Subnetwork Approach to Earthquake Early Warning. *Bull. Seism. Soc. Am* , 92 (5): 2008-2018.